View metadata, citation and similar papers at core.ac.uk

brought to you by CORE

provided by Elsevier - Publisher Connector

Available online at www.sciencedirect.com

ScienceDirect

Developmental Biology 298 (2006) 458–469

DEVELOPMENTAL BIOLOGY

www.elsevier.com/locate/ydbio

Transmission of modified nucleosomes from the mouse male germline to the zygote and subsequent remodeling of paternal chromatin

G.W. van der Heijden [a,1], A.A.H.A. Derijck [a,1], L. Ramos [a], M. Giele [a], J. van der Vlag [b], P. de Boer [a,*]

[a] *Department of Obstetrics and Gynaecology, Radboud University Nijmegen Medical Centre, P.O. Box 9101, 6500 HB Nijmegen, The Netherlands*

[b] *Nephrology Research Laboratory (279), Nijmegen Centre for Molecular Life Sciences and Division of Nephrology, Radboud University Nijmegen Medical Centre, P.O. Box 9101, 6500 HB, Nijmegen, The Netherlands*

Received for publication 2 March 2006; revised 27 June 2006; accepted 30 June 2006
Available online 7 July 2006

Abstract

Rapidly after gamete fusion, the sperm nucleus loses its specific chromatin conformation and the DNA is repopulated with maternally derived nucleosomes. We evaluated the nature of paternally derived nucleosomes and the dynamics of sperm chromatin remodeling in the zygote directly after gamete fusion. We observed histone H4 acetylated at K8 or K12 already prior to full decondensation of the sperm nucleus, suggesting that these marks are transmitted by the spermatozoon. Tracking down the origin of H4K8ac and H4K12ac during spermiogenesis revealed the retention of nucleosomes with these modifications in the chromocenter of elongating spermatids. We show that sperm constitutive heterochromatin is enriched for nucleosomes carrying specific histone modifications which are transmitted to the zygote. Our results suggest an epigenetic mechanism for inheritance of chromosomal architecture. Furthermore, up to pronucleus formation, histone acetylation and phosphorylation build up in a cascade-like fashion in the paternal chromatin. After formation of the pronucleus, a subset of these marks is removed from the heterochromatin, which suggests a reestablishment of the euchromatin–heterochromatin partition.
© 2006 Elsevier Inc. All rights reserved.

Keywords: Spermiogenesis; Germline; Zygote; Pre-implantation; Chromatin; Heterochromatin; Epigenetics; Histone acetylation; Histone phosphorylation

Introduction

In the condensed sperm nucleus, DNA is present in an inert, sperm-specific constitution, in which it is bound to protamines that facilitate a high density packing (Ward and Coffey, 1991). During spermiogenesis, the replacement of histones by protamines is not complete and varies strongly among species. In mouse sperm, an estimated 1% of the DNA remains bound to nucleosomes (R. Balhorn, personal communication). The nuclear organization of the sperm genome is well defined, with the telomeres positioned at the outer membrane and centromeric (constitutive) heterochromatin in the center of the nucleus, in sperm also referred to as the chromocenter (Haaf and Ward, 1995).

After fusion of mammalian gametes, the start of development is characterized by the resumption of meiosis of the arrested secondary oocyte and the transformation of the sperm nucleus into the male pronucleus (PN) (Sutovsky and Schatten, 2000; Wright, 1999). A sea change in paternal chromatin conformation takes place directly after oocyte penetration, swiftly resulting in the reestablishment of nucleosomal chromatin (van der Heijden et al., 2005). During the first hours after gamete fusion, the paternal chromatin is not yet engulfed by a nuclear membrane. It is only after approximately 3 h, when the paternal chromatin has expanded once more after a period of recondensation, that the nuclear membrane can be detected and the male PN is defined (Adenot et al., 1991).

Relatively little is known of the pre-PN phase during which the paternal genetic contribution becomes intertwined with maternal processing. The transformation from the sperm-specific chromatin conformation to a somatic-like chromatin architecture is fast. Already in G1, paternal chromatin can be

* Corresponding author. Fax: +31 243668597.
E-mail address: P.deboer@obgyn.umcn.nl (P. de Boer).
[1] Both authors contributed equally.

0012-1606/$ - see front matter © 2006 Elsevier Inc. All rights reserved.
doi:10.1016/j.ydbio.2006.06.051

triggered to undergo chromosome contraction (Dyban et al., 1993). Whether the remaining ~1% nucleosomal chromatin plays a facilitating role in this reconfiguration is unknown. In human sperm, telomeres and centromeres contain nucleosomal chromatin (Palmer et al., 1990; Zalenskaya et al., 2000), possibly indicating that preservation of nucleosomal domains is important. The rapid return of "somatic" chromatin characteristics is also illustrated by the biphasic replication pattern observed in the paternal PN during zygotic S-phase, indicating that euchromatin is already distinguished from late replicating heterochromatin (Aoki and Schultz, 1999). In somatic nuclei, these types of chromatin differ in histone lysine methylation patterns (Peters et al., 2003). Paternal zygotic chromatin virtually lacks all of these post-translational modifications (PTMs) (Cowell et al., 2002; Kourmouli et al., 2004; van der Heijden et al., 2005).

It has been reported that, prior to full decondensation, the paternal chromatin undergoes rapid acetylation of histone H4 at lysine 5, indicating that histone acetylation might play an important role in early zygotic development (Adenot et al., 1997). To gain a better insight into the nature and dynamics of paternal chromatin remodeling in the early zygote, we evaluated the appearance of histone PTMs that were known to be present during zygotic S phase/G2 phase (Kim et al., 2003; Stein et al., 1997). We observed a stepwise appearance of maternally derived histone PTMs in the pre-PN chromatin. In several cases, this was followed by a partial or complete removal when the PN had formed, which indicated that these processes are dynamic and follow a developmental program. Furthermore, we identified the chromocenter of the decondensing sperm nucleus as a region enriched for modified nucleosomes. It is well established that, during the first hours after gamete fusion, DNA methylation is actively removed from the paternal euchromatin, while being preserved in the heterochromatin (Santos et al., 2005). We speculate that nucleosomal chromatin in the sperm chromocenter facilitates the difference in demethylation pattern.

By revealing the localization of these modified nucleosomes in the chromocenter of elongating spermatids and sperm, we demonstrate that nucleosomal chromatin originating from the male germline contributes to the zygote. Our results increase the notion that sperm contributes more than only its genetic content.

Materials and methods

Gamete collection and IVF

IVF was performed as described previously (van der Heijden et al., 2005). Briefly, sperm was obtained from CBA/B6 F1 mice (6–20 weeks). Caudae epididymis were partially cut open to allow swimming-out of sperm. For capacitation, the sperm suspension was transferred to the bottom of a 5 ml tube with HTF 3% BSA, including 10 μM adenosine. The sperm suspension was incubated at 37°C, 5% CO_2 in air for 1 h. At 45 min, a sperm count was performed. Female B6/CBA F1 mice (4–12 weeks old) were housed with adjusted light periods set at 9:00–21:00 h. Superovulation was induced by injecting 7.5 U PMSG (Intervet, Boxmeer, The Netherlands) around 18:00 h and 7.5 U HCG (Intervet) 48 h later. Females were sacrificed next morning at 9:00 h. Oocytes were harvested from the ampullae and transferred to 50 μl HTF 0.5% BSA droplets covered with light mineral oil. Sperm was added to these droplets to a final concentration of $1*10^6$ cells/ml.

Timing of zygote development

The timing of gamete fusion and subsequent zygote development in our IVF setting has been described earlier (van der Heijden et al., 2005). Oocyte penetration occurs predominantly 70 min post-insemination (pi). For this study, zygotes were fixed at four time points pi: 70, 100, 150 and 280 min, respectively. All time periods mentioned in this report are corrected for the 70-min lag phase.

Antibodies

The following antibodies were used: from Upstate Biotechnology (Lake Placid, USA): H3S10ph (06-570; 1:1000 dilution), H3K9K14ac (06-599, 1:500), H3K18ac (07-354; 1:500), H4K5ac (06-759; 1:50), H4K8ac (06-760; 1:1000), H4K12ac (06-761; 1:500) and H4K16ac (06-762; 1:500). Antibodies against protamines: HuP1N, HuP2B (R. Balhorn; 1:1000). Antibodies #32, #34 and #36 are monoclonal autoantibodies derived from lupus mice: #32 is nucleosome-specific (1:3000) (Kramers et al., 1996), #36 is specific for dsDNA (1:800) (Losman et al., 1992) and #34 is specific for the replication histone H3 variants H3.1 and H3.2 (1:1500) (van der Heijden et al., 2005). Furthermore, antibodies against HP1-α (P. Singh; 1:200), HP1-β (P. Singh; 1:100), H3K9me3 and H4K20me3 (T. Jenuwein; 1:250), Hira (D34, P. Adams; 1:100) and CREST (P. Burgoyne; 1:5000).

Secondary abs that were used: Molecular Probes, Oregon, USA: A11001 Fluor 488 goat anti-mouse IgG (H+L), A11012 Fluor 594 goat anti-rabbit IgG (H+L), Sigma: F6258; anti-rat IgG, FITC-conjugated. All were used in a 1:500 dilution. All secondary abs were tested for non-specific binding, which was never observed.

Immobilization, fixation and immunofluorescence staining of zygotes

Before fixation of the zygotes, the zona pellucida was removed using acidic tyrode (pH 2.5) containing 1% BSA. Thereafter, cells were immobilized in a fibrin clot (Hunt et al., 1995). Fibrinogen was obtained from Calbiochem (cat. nr. 341573), and thrombin was obtained from Sigma (cat. nr. T-6634). Cells were fixed in 2% paraformaldehyde (PFA), 0.15% Triton X-100 for 30 min. Immunofluorescence (IF) was applied as described before (Baart et al., 2000).

Preparation of nuclear spreads from the testis and characterization of spermatid stages

Spreads were obtained as described with minor modifications (Peters et al., 1997). Testes of CBA/B6 F1 mice (12 weeks old) were dissected and placed in MEMα-HEPES. After removal of the tunica albuginea, the tubuli were minced between two curved forceps. The cell suspension was transferred to a 10 ml tube filled with MEMα. After a quick spin at 400 rpm (~13.5×*g*), the supernatant was collected in a clean tube and centrifuged for 10 min at 1000 rpm (~84×*g*). The supernatant was removed up to ~1 ml, the pellet suspended and MEMα added. This step was repeated twice. After resuspending the pellet, an equal volume of hypobuffer (17 mM sodium citrate; 50 mM sucrose; 30 mM Tris–HCl pH 8.2) was added and cells were incubated for 8 min followed by centrifugation as before (~1000 rpm). The supernatant was removed, and the pellet was carefully resuspended in 1–2 ml 100 mM sucrose. Ten microliters of this suspension was applied to a PFA-coated glass slide (1% PFA, 0.15% Triton X-100, pH 9.2–9.5). The cells were kept for 2 h in a humidified atmosphere. After 1.5 h, the box was opened and slides were washed with 0.08% photoflow (Kodak). IF was performed as described above. Because spermatid nuclei were observed outside their cellular organization, spermatid development steps were appointed according to the criteria of Russell et al. (1990). For every ab tested, at least 150 nuclei were evaluated.

Decondensation of mouse caput sperm

The epididymis was cut open and sperm was allowed to swim out in PBS. The sperm pellet (3000 rpm, 8 min in an Eppendorf bench centrifuge) was resuspended in 50 μl PBS (pH 7.0). The suspension was diluted 1:4 in water, and drops of 5 μl were placed on a glass slide and dried. One hundred microliters of decondensing mix (freshly prepared 25 mM DTT, 0.2% Triton X-100, 200 IU heparin/ml (Leo Laboratories) in PBS) was put on top of the dried sperm followed by incubation in a humidified atmosphere for 15–18 min. The speed and degree of decondensation were followed by phase contrast microscopy. When the majority of the nuclei appeared dull gray with roughly twice the surface area of the undecondensed sperm heads, the slide was placed in a coplin jar with 4% PFA in PBS (pH 7) for 15 min. Subsequently, slides were washed in PBS and dried. IF was performed as described above. For every staining, at least 150 nuclei were evaluated.

Collection of images

Images were collected with a Zeiss Axioplan fluorescence microscope. Pictures were captured by a Zeiss AxioCam MR camera with Axiovision 3.1 software (Carl Zeiss). Shown images of type *a*, *b*, *c* post-penetration sperm nuclei and PNs are either stacks projected into a single image or a single slide of a stack. Whenever necessary, images where deconvoluted with Metamorph software version 6.

Results

Stepwise appearance of histone modifications in the paternal chromatin

Using specific antibodies, we determined the appearance of acetylated histone H3 and H4 isoforms in paternally derived chromatin of the early zygote at four time points after insemination. As described earlier (van der Heijden et al., 2005), we could distinguish three types of paternal nuclei in the pre-PN zygote: (1) type *a* nuclei, which are partially decondensed, hence contain both condensed and decondensed chromatin; (2) type *b* nuclei, which are fully decondensed; and (3) type *c* nuclei, which are recondensing (Figs. 1A, C, D, respectively). Decondensation of sperm chromatin always commenced in the posterior and ventral parts and spread to the tip, which expanded last (Figs. 1A, B).

H4K8ac

Acetylated histone H4 at K8 was consistently observed from the initial stages of sperm chromatin expansion on. Strikingly, in type *a* nuclei, this mark was restricted to the center region (Figs. 1A, B). In type *b* nuclei, H4K8ac localized to the chromocenter (Fig. 1C). To confirm this colocalization, we performed double stainings with the kinetochore-specific CREST serum. The kinetochores were indeed embedded in chromatin regions intensely stained by the H4K8ac ab (Figs. 1F–H). This was different from somatic cells, where heterochromatin was characterized by a low abundance of histone acetylation (Figs. 1I–I″). The restricted localization in type *a* and *b* nuclei was masked after full decondensation due to increasing levels of maternally derived H4K8ac (Fig. 1D). The global localization of H4K8ac became more restricted after formation of the PN, when the signal disappeared from heterochromatin areas surrounding prenucleoli (Arney et al., 2002) (Fig. 1E).

H4K12ac

Overall, in the pre-PN phases, a steady increase of the signal for H4K12ac was observed (Figs. 1J–M). In the early decondensing regions, the signal was already detected (Fig. 1J). In type *b* nuclei, a prominent appearance of H4K12ac was observed in the posterior rim and, to a lesser extent, in the chromocenter (Fig. 1K). The signal was always less intense or even absent in the anterior regions of early type *b* nuclei (Fig. 1K). A steady increase of signal intensity, however, could be detected in these regions at a later stage (Fig. 1L). During recondensation of the sperm chromatin, H4K12ac was homogeneously present (Fig. 1M). In the PN, H4K12ac, alike H4K8ac, disappeared from the peri-prenucleolar chromatin (Fig. 1N).

Maternally derived, newly incorporated histone H4, acetylated at K5 and K12 (Sobel et al., 1995), provides an opportunity to distinguish deposited maternal nucleosomes from paternal ones that lack these marks. In order to detect chromatin regions populated by paternally derived nucleosomes, we performed double stainings with a nucleosome-specific ab (#32) combined with the H4K12ac ab. Indeed, at the earliest phase of decondensation, we could observe regions containing nucleosomal chromatin that was not acetylated at K12 (Fig. 1O). However, the subsequent appearance of H4K12ac obscured these regions quickly (Fig. 1P).

H3S10ph, H4K16ac, H3K9K14ac and H3K18ac

With regard to time of appearance, di-acetylated histone H3 at K9 and K14 (H3K9K14ac), acetylated histone H3 at K18 (H3K18ac), acetylated histone H4 at K16 (H4K16ac) and phosphorylated histone H3 at S10 (H3S10ph) were distinct from H4K8ac and H4K12ac since they were not observed in type *a* nuclei (data not shown). H3S10ph and H4K16ac were first observed at complete decondensation (type *b* nuclei) around 30 min after gamete fusion. The marks localized to the periphery and chromocenter of the type *b* decondensing sperm nucleus (Figs. 2A–A′ and D–D′).In time, the signal for both marks progressed until it covered the entire paternal chromatin (Figs. 2B–B′ and E–E′). A rapid decline of signal for the two marks was observed at PN formation. For H3S10ph, the overall signal decreased and bright foci were left (Figs. 2C–C′). Finally, this mark completely disappeared when prenucleoli were pronounced, approximately 210 min after gamete fusion. At this stage, H4K16ac had not vanished totally but was present in a more granular pattern (Figs. 2F–F′). We observed a synchronized appearance of H3K9K14ac and H3K18ac shortly after H3S10ph and H4K16ac became detectable. These histone PTMs did not concentrate in the chromocenter but were initially observed faintly throughout the sperm chromatin (Figs. 2G–G′ and J–J′). In type *c* nuclei, these marks were more abundant (Figs. 2H–H′ and K–K′). This increase continued throughout PN formation (Figs. 2I–I′ and L–L′).

Localization of nucleosomes, protamines, modified histones H3 and H4 and HP1 during spermiogenesis

As described above, H4K12ac and especially H4K8ac were observed immediately after gamete fusion. We investigated the

possibility of their presence in the sperm nucleus prior to fertilization. To this end, spreads were made from mouse spermatogenic cells and used for IF staining. Since progressive compaction of sperm chromatin during spermiogenesis is likely to interfere with penetration of antibodies, we investigated until which morphological nuclear step IF detection was feasible. By

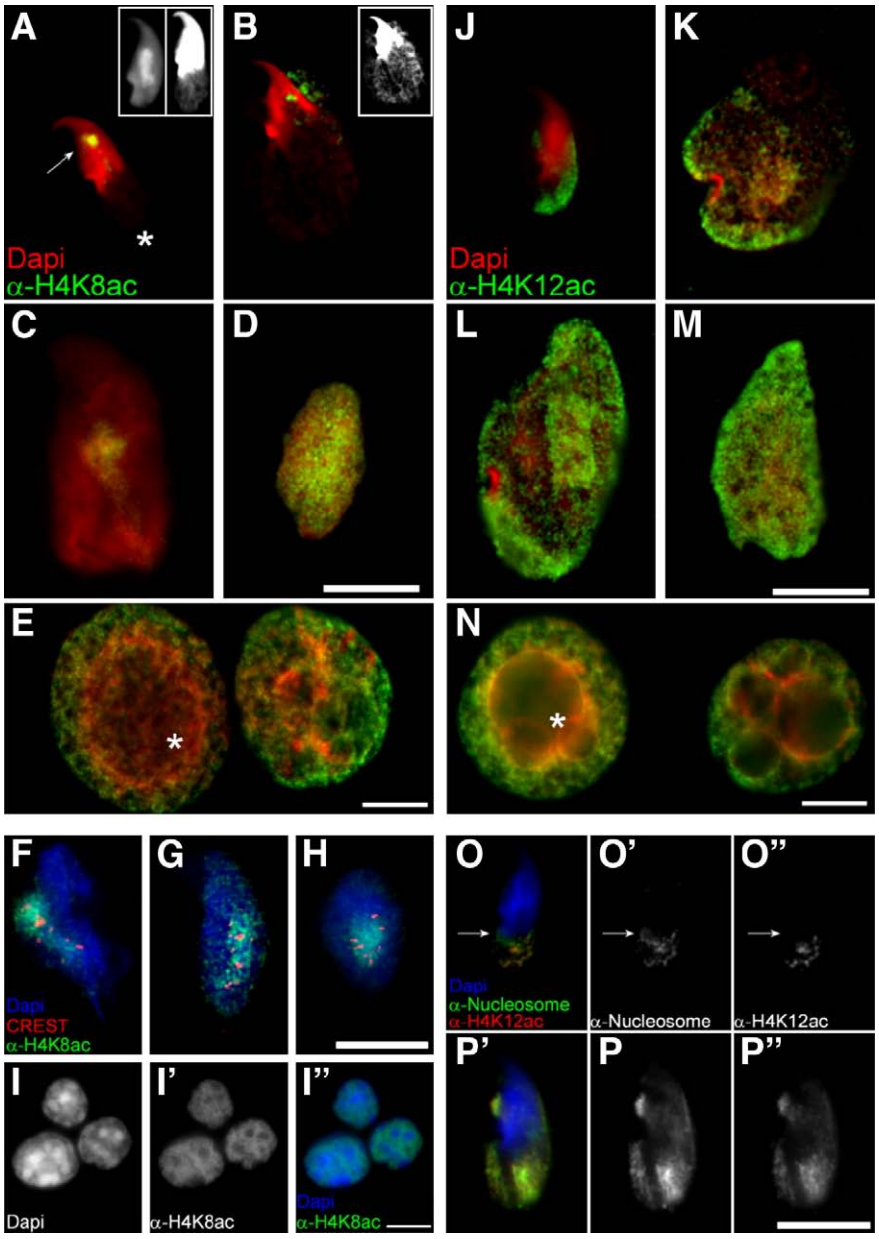

Fig. 1. Localization of H4K8ac and H4K12ac in the zygotic male chromatin. (A–E) Localization of H4K8ac in type *a* nuclei (A, B; $n=19$), type *b* nuclei (C; $n=47$), type *c* nuclei (D; $n=17$) and in the PN (E; $n=52$) (see Results section for the description of *a*, *b* and *c* stages). DAPI is pseudo-colored red, and H4K8ac is depicted in green. All pictures are cutouts from whole zygote images. Rapidly after the fusion of oocyte and sperm, decondensation of the nucleus starts. This caused the rim of the sperm nucleus to blur (compare DAPI staining inset in panel A of a sperm nucleus (left) with the decondensing sperm nucleus (right)). This process was always first observed in the posterior and center regions, indicated in panel A with an asterisk and an arrow, respectively. The left inset in panel A also illustrates the localization of the chromocenter. In the PN (E), H4K8ac was reduced in the heterochromatic regions around the prenucleolus (denoted by asterisk). The left PN is the paternal one, the right PN is maternal. (F–H) The H4K8ac positive domain embeds the centromeres in type *b* nuclei. Double staining with the kinetochore CREST ab in red and α-H4K8ac in green. DAPI is pseudo-colored blue ($n=8$). (I–I″). In somatic mouse follicle cells, heterochromatin domains are DAPI bright (I). These regions contained low levels of H4K8ac (I′). (J–N) Localization of H4K12ac in type *a* sperm nuclei (J; $n=28$), type *b* nuclei (K, L; $n=43$), type *c* nuclei (M; $n=14$) and in the early PN (N; $n=18$). DAPI is pseudo-colored red and H4K12ac green. Alike H4K8ac, this mark was present as soon as technically could be observed. In contrast to H4K8ac, it spreads across the decondensing sperm chromatin immediately (J, K, L). In the PN, H4K12ac was reduced in the heterochromatic regions around the prenucleolus (denoted by asterisk). The left PN is the paternal one, the right PN is maternal. (O–O″, P–P″) Double staining with a nucleosomal ab (#32) and H4K12ac ab to pinpoint regions populated by paternally derived nucleosomes ($n=12$). Localization of nucleosomes (O′, P′) and H4K12ac (O″, P″) in type *a* nuclei (O, P, merge with DAPI pseudo-colored blue, the nucleosomal ab in green and H4K12ac in red). The progression of chromatin decondensation was clearly visible when comparing (O), which only underwent some posterior decondensation and (P), where decondensation was clearly more advanced in the posterior region and was also observed in the mid-ventral region. The arrow in panels O–O″ points at a region where nucleosomes are present without H4K12ac acetylation. Scale bar represents 10 μm.

staining with a dsDNA ab (#36), we observed lack of signal in the anterior region of a nuclear morphology, roughly coinciding with step 12 (Supplementary Fig. 1) but not in preceding nuclear forms. The partial penetration of elongated spermatids by the dsDNA ab reflected the progression of nuclear remodeling along the anterior–posterior axis (Hazzouri et al.,

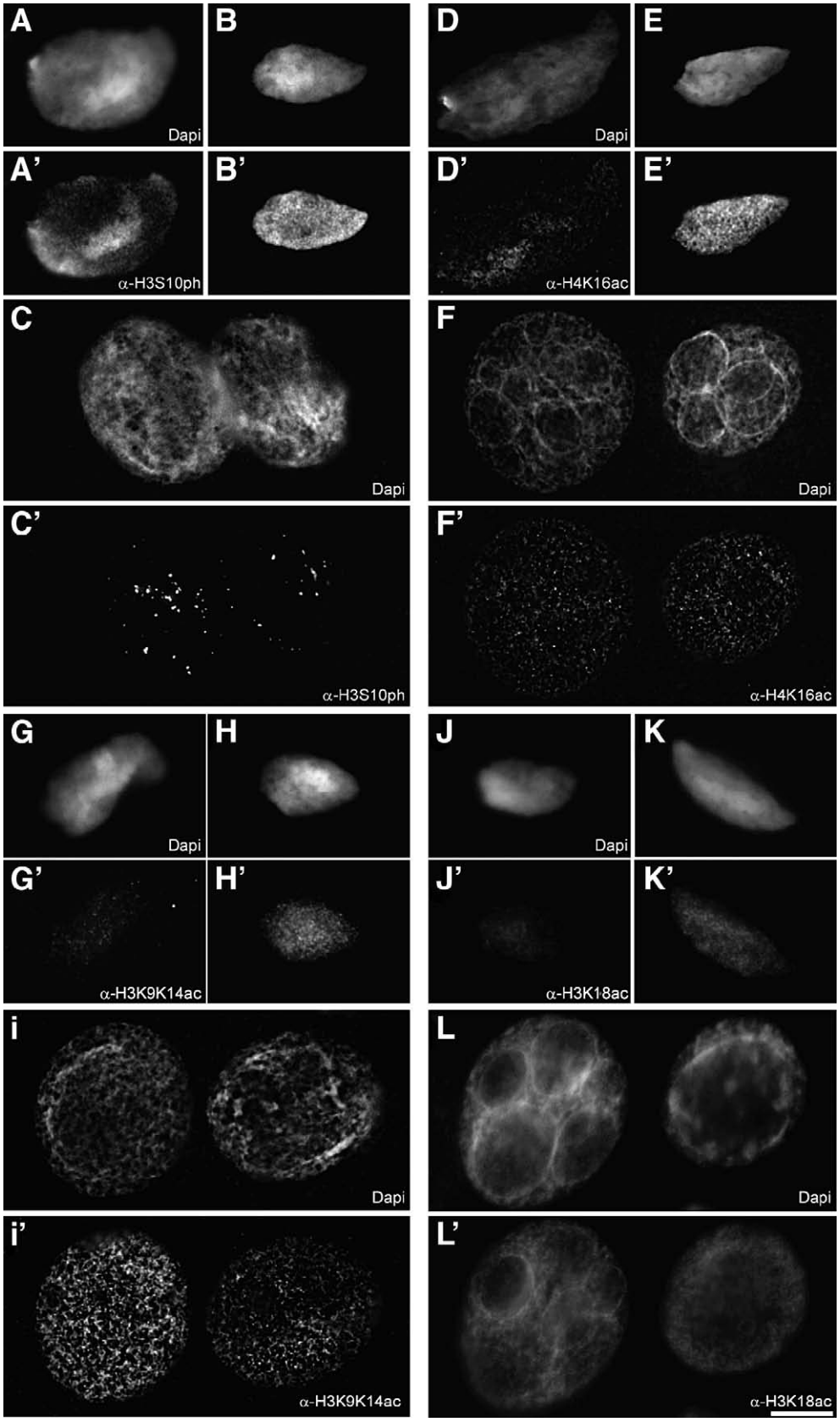

2000). Since DAPI has a preference for AT-rich sequences, as mouse centric DNA is, these domains were more brightly stained.

Nucleosomes and protamines

Staining of elongating spermatids with a nucleosome-specific ab (#32) visualized the process of their removal. It also revealed a gradually appearing difference between euchromatin and heterochromatin. At morphologies representative for step 9, nucleosomes were generally evenly present (Figs. 3A–A″). In more differentiated spermatids, a selective reduction of the overall signal was observed. Regions with a higher intensity colocalized with the chromocenter, whereas nucleosome levels in the surrounding chromatin were greatly diminished (Figs. 3B–B″). Staining with the dsDNA ab showed a relatively homogeneous signal in elongating spermatids with a corresponding morphology (Supplementary Fig. 1). The higher concentration of nucleosomes in the chromocenter is therefore not due to an elevated DNA concentration.

During further differentiation, a progressive reduction of nucleosomes was observed. However, even in step 11 spermatid nuclei, a signal could still be observed in the chromocenter (Figs. 3C–C″). This also applied to the posterior region of the nucleus (Figs. 3C–C″). Since chromatin remodeling proceeds in the anterior–posterior axis, this may be expected. To establish whether the nucleosomes observed in the chromocenter were newly deposited onto the DNA, we investigated whether de novo nucleosome deposition took place. Since DNA replication does not occur during spermiogenesis, all newly deposited nucleosomes will involve the histone chaperone Hira, which specifically deposits histone H3.3–H4 dimers on the DNA (Tagami et al., 2004). Staining with a Hira-specific ab revealed that this protein is not present in elongating spermatid nuclei, which implies the lack of de novo nucleosome deposition (data not shown).

The presence of nucleosomes in the chromocenter should lead to a lower protamine (Prm) content in this region since they compete for DNA binding. Indeed, staining with Prm1 and 2-specific abs revealed a reduced signal in the chromocenter (Figs. 3D–D″).

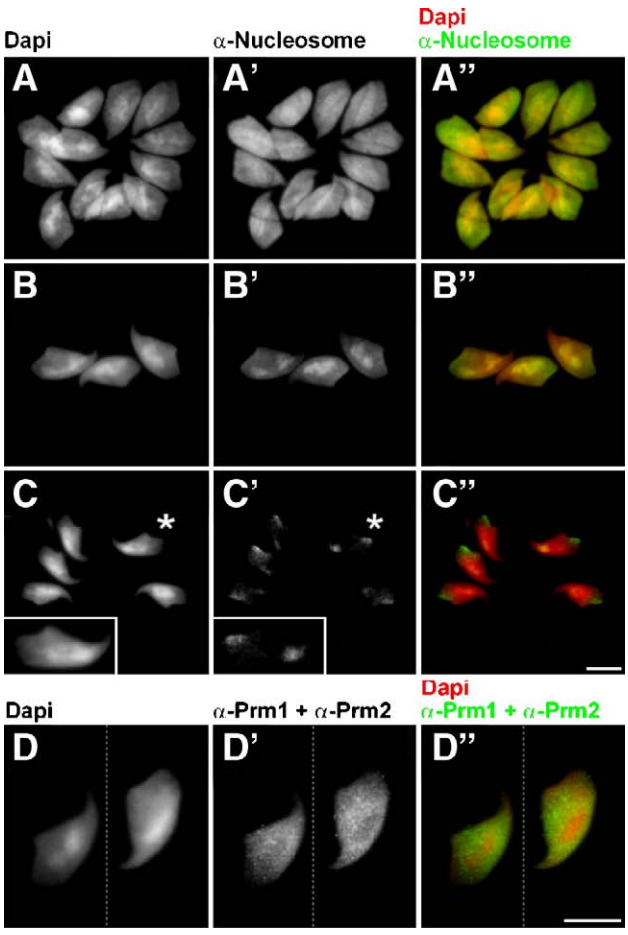

Fig. 3. Localization of nucleosomes and protamines in spermatids. The left column depicts DAPI, the middle column ab staining and the right column the merged image. DAPI is pseudo-colored red, the ab signal is in green. (A–C″) Localization of nucleosomes by ab #32 in spermatids in advancing stages of condensation. A relative enrichment of nucleosomes in the chromocenter could be observed. In panels A–A″ (morphologies representing steps 9/10), DAPI-bright regions did not necessarily colocalize with bright ab staining. In later stages (morphology step 10), there is a clear colocalization of the two (B–B″). After further advancement of chromatin condensation (morphology step 11), nucleosomes could still be observed in the chromocenter (C–C″). Inset is a magnification of the nucleus marked with an asterisk. (D–D″) Localization of both Prm1 and Prm2 in elongating sperm nuclei in morphology step 10. A lower concentration of protamines was observed in the chromocenter, most likely the result of the presence of nucleosomal bound DNA. A mixture of both abs was used. Scale bar represents 10 μm.

Acetylated isoforms of histone H4

At initial stages of nuclear elongation, a homogeneous localization of H4K5ac, K8ac, K12ac and K16ac throughout the spermatid nucleus was observed (Figs. 4.1A–A″, D–D″ and Supplementary Fig. 2) as has been described for whole mount seminiferous tubuli earlier (Hazzouri et al., 2000). At later stages (morphological steps 10–11), however, H4K5ac and H4K16ac were severely reduced or had completely disappeared (Figs. 4.1E–E″; F–F″ and Supplementary Fig. 2). H4K8ac and K12ac exhibited the same behavior as nucleosomes and were lost from euchromatin but retained in the chromocenter and the posterior region (Figs. 4.1A–C″ and Supplementary Fig. 2).

H3K9me3, H4K20me3 and HP1

In a previous study (van der Heijden et al., 2005), we did not detect the characteristic heterochromatin marks H3K9me3 and

Fig. 2. Localization of H3S10ph, H4K16Ac, H3K9K14ac and H3K18ac in the zygotic male chromatin. (A–C, A′–C′) DAPI and corresponding α-H3S10ph staining in type *b* sperm nucleus (A and A′; $n=17$), type *c* sperm nucleus (B and B′; $n=16$) and in the PN (C and C′; $n=25$). H3S10ph had completely disappeared when prenucleoli had formed. (D–F, E′–F′) DAPI and corresponding α-H4K16ac staining in type *b* sperm nucleus (D and D′; $n=16$), type *c* sperm nucleus (E and E′; $n=13$) and in the PN (F and F′; $n=12$). (G–I, G′–I′) DAPI and corresponding α-H3K9K14ac staining in type *b* sperm nucleus (G and G′; $n=25$), type *c* sperm nucleus (H and H′; $n=9$) and in the PN (I and I′; $n=15$). (J–L, J′–L′) DAPI and corresponding α-H3K18ac staining in type *b* sperm nucleus (3J and J′; $n=10$), type *c* sperm nucleus (K and K′; $n=7$) and in the PN (L and L′; $n=12$). In all cases, the left PN is the paternal one, the right PN is maternal. Scale bar represents 10 μm.

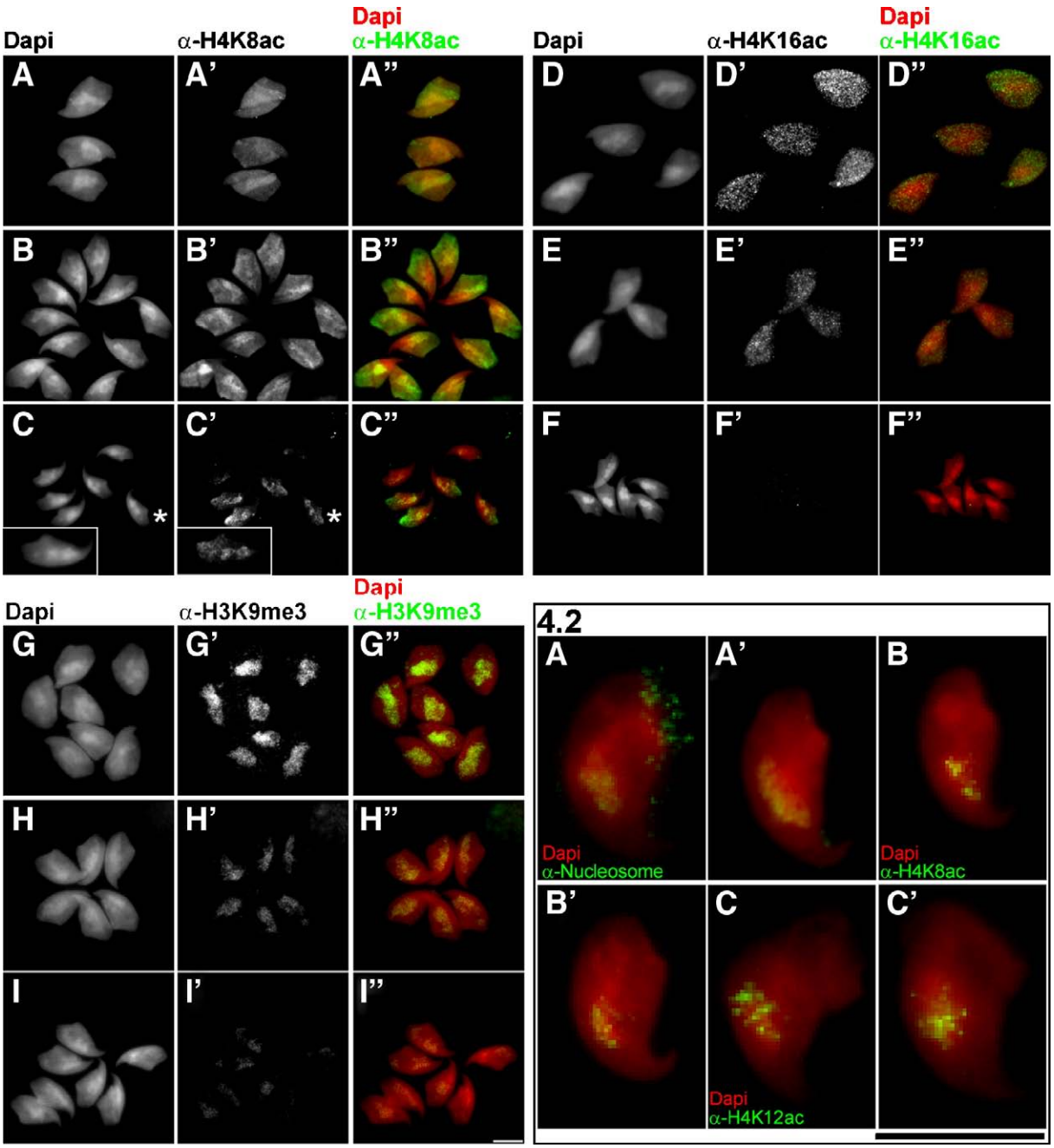

Fig. 4. (1) Localization of H4K8ac, H4K16ac and H3K9me3 in spermatid nuclei. The left column depicts DAPI, the middle column ab staining and the right column the merged images. DAPI is pseudo-colored red, the ab signal is in green. (A–C″) Localization of H4K8ac in spermatids in advancing stages of elongation. Higher H4K8ac levels were sometimes observed in regions encompassing euchromatin and heterochromatin in morphologies representing step 10 (A–A″). Later on the signal was concentrated in the chromocenter, though the colocalization was not absolute in morphologies representing step 11 (B–B″). In spermatids that experienced further nuclear condensation (morphologies representing step 12 and beyond), signal was mainly observed in the posterior region but also in the more anteriorly localized chromocenter (C–C″). Inset is a magnification of the nucleus marked with an asterisk. A similar pattern was observed for H4K12ac (Supplementary Fig. 2). (D–F″) Localization of H4K16ac in spermatids in advancing stages of elongation. Initially, H4K16ac was observed homogeneously throughout the spermatid nucleus (morphologies representing steps 9/10, D–D″). In spite of progressive condensation (E–E″), the signal was slightly reduced, indicating removal of this mark. At a later stage (morphologies representing step 11), when ab penetration was still possible, the mark had disappeared (F–F″). A similar pattern was observed for H4K5ac (Supplementary Fig. 2). (G–I″) Localization of H3K9me3 in spermatids in advancing stages of elongation. A clear colocalization of this mark with the chromocenter was observed in all stages (morphologies representing steps 9/10; G–G″ and 10; H–H″). Reduction of the signal was apparent with increase of condensation (morphologies representing steps 10/11; I–I″). A similar pattern was observed for H4K20me3 (Supplementary Fig. 3). Scale bar represents 10 μm. (2) Localization of nucleosomes, H4K8ac and H4K12ac in sperm nuclei. Localization of nucleosomes (A, A′), H4K8ac (B, B′) and H4K12ac (C, C′) in artificially expanded sperm nuclei derived from the caput epididymis. Signal was observed in the chromocenter. DAPI is pseudo-colored red, the ab signal is in green. Scale bar represents 10 μm.

H4K20me3 in pre-PN stage paternal zygotic chromatin. H3K9me3 serves as a binding site for HP1, a protein also able to bind to itself, thereby inducing chromatin compaction (Singh and Georgatos, 2002). Absence of these marks in type *a* and *b* zygotic sperm chromatin indicated that these were removed from heterochromatin during spermiogenesis. Since this did not seem to be the case for H4K8ac and K12ac, we determined when these heterochromatin markers were lost from spermatid nuclei. H3K9me3 and H4K20me3 were clearly present in spermatids after the onset of elongation (Figs. 4.1G–G″ and Supplementary Fig. 3). A clear colocalization of both marks with the DAPI-bright chromocenter was observed. With progression of elongation, intensity levels were reduced. At morphologies around step 11, signals for both marks were highly reduced or virtually absent, following the same dynamics as H4K5ac and H4K16ac. HP1-α was lost from spermatid nuclei prior to the disappearance of tri-methylations (data not shown), whereas HP1-β quickly disappeared after the onset of spermatid nuclear elongation (Supplementary Fig. 3), but a faint signal could be observed in spermatids that had progressed to morphology step 12. This fits with the reported presence of HP1-β in mouse sperm as determined by Western blot analysis (Hoyer-Fender et al., 2000).

Localization of nucleosomes, H4K8ac and H4K12ac in mature sperm

To be certain that nucleosomes and modified histone H4 were also present upon completion of spermiogenesis, we analyzed gametes derived from the caput epididymis. After in vitro chromatin decondensation, a prominent signal in the anterior central region of the nucleus was observed for nucleosomes, H4K8ac and H4K12ac (Figs. 4.2A–C). In all cases, the signals colocalized with the chromocenter. These results resemble our observations in late elongating spermatids. Occasionally, the nucleosome-specific ab also stained the rim of the sperm nucleus, possibly reflecting the findings of Pittoggi et al. (1999). The posterior localization of nucleosomes in spermatid nuclei (Figs. 3C–C″) was not observed in sperm nuclei, which may indicate their eventual removal during spermiogenesis.

Discussion

Centric DNA in sperm is enriched for nucleosomes

In mouse sperm, about 1% of the DNA is wrapped around nucleosomes (R. Balhorn, personal communication). These nucleosomes are not randomly distributed over the sperm DNA. In a previous report, it was shown that retroposon sequences show enrichment for nucleosomes and that these sequences are localized in the nuclear periphery (Pittoggi et al., 1999). Here, we describe a clear enrichment of nucleosomal chromatin in centric "heterochromatin" DNA of mouse sperm (Fig. 4.2). Pittogi and coworkers communicated that their fraction of DNA in a nucleosomal conformation did not exceed 0.1% (Pittoggi et al., 1999). We propose, therefore, that a major portion of the remaining nucleosomal chromatin in mouse sperm is contained in the centric heterochromatin.

Hypoacetylation of histone H4 correlates with nucleosome retention

During mouse spermiogenesis, histones are stepwise replaced by protamines (for a review, see Rousseaux et al., 2005). We observed that nucleosome density in euchromatin was declining faster than in the chromocenter where nucleosomes can still be detected when nuclear elongation proceeds (Figs. 3A, B). Since de novo nucleosome assembly does not take place, these nucleosomes must be retained from the original chromatin.

A similar pattern of selective preservation during spermiogenesis was observed for two specific acetylated H4 isoforms, H4K8ac and H4K12ac. Whereas H4K5ac and H4K16ac eventually disappeared completely from the spermatid chromatin, H4K8ac and H4K12ac levels were drastically, but not entirely, reduced and restricted to the chromocenter and posterior region (Fig. 4 and Supplementary Fig. 2). Like the retained nucleosomes, these histone PTMs are set prior to the onset of nucleosome eviction since histone acetylation does not take place in condensing spermatids (Hazzouri et al., 2000). Hyperacetylation of the nucleosome and especially histone H4 is well documented during spermiogenesis and has been observed in several species (Rousseaux et al., 2005). Acetylation partially neutralizes the positive charge of the histone tail and will therefore weaken DNA–nucleosome and nucleosome–nucleosome interactions, inducing a more open chromatin structure (Sterner and Berger, 2000), which may then facilitate removal of nucleosomes and subsequent replacement by protamines (Oliva et al., 1987). On the protein level, it has been shown that Brdt, identified as a testis-specific chromatin reorganizer, needs a certain degree of histone acetylation for proper function (Pivot-Pajot et al., 2003). If hyperacetylation is beneficial for nucleosome eviction, a hypoacetylated state might help to retain nucleosomes. Notably, nucleosomes in the chromocenter and the posterior region of the spermatids were not hyperacetylated (lacking at least H4K5ac and H4K16ac; Fig. 4F and Supplementary Fig. 2C). However, nucleosomes disappeared from the posterior region of the nucleus, indicating that hypoacetylation alone is not sufficient for retention in the chromocenter. It has been shown that also the higher AT content of centric heterochromatin contributes to intrinsic nucleosome stability (Widlund et al., 1997). Possibly, the accumulative effect of a lower acetylation level and a more stable nucleosome conformation hampers nucleosome disassembly, resulting in nucleosome retention in the chromocenter.

Potential role of transmitted male nucleosomes

When premature chromosome condensation is induced in G1 pronuclear zygotes, the paternal and maternal chromatin is reconfigured into mitotic chromosomes (Dyban et al., 1993), displaying centric heterochromatin. Apparently, chromosome architecture is already reestablished during zygotic G1.

Structural domains as telomeres, centromeres and centric heterochromatin have distinct roles in chromosomal organization. Manipulation of these domains, if at all possible, often results in genome instability (de Lange, 2002; Peters et al., 2001). Remarkably, telomeres and centromeres are reported to be arranged into nucleosomal chromatin in human sperm (Palmer et al., 1990; Zalenskaya et al., 2000). The localization of telomeres in the nucleosome-rich nuclear periphery in mouse sperm (Haaf and Ward, 1995) and the presence of the kinetochore-specific CREST signal in the chromocenter of elongating spermatids (data not shown) and shortly after gamete fusion suggest a similar organization in mouse. Hence, also in mouse sperm, it seems that structurally important chromosome domains maintain to some degree a nucleosomal chromatin conformation.

The organization of telomeric and centric DNA into nucleosomes could serve as a chromatin blueprint, directing the remodeling machinery by supplying a nucleosomal template. Additionally, the presence of acetylated lysines in the histone tails – e.g., H4K8ac and H4K12ac – could provide an incentive for binding chromatin remodelers via their bromodomains, typically contained in chromatin-associated proteins (Yang, 2004).

It has been that shown that telomere length is pivotal for proper early zygote development (Liu et al., 2002). When sperm of 3rd generation telomerase knock out males fertilize wild type oocytes, a high percentage of zygotes fails to undergo cleavage. In these zygotes, the sperm nucleus does not decondense, implying a structural role for telomeres during early sperm chromatin remodeling. The complex nature of centric heterochromatin and centromeres will make it difficult to determine whether this also applies to them.

The finding by Santos et al. (2005) that centric DNA is protected from genome-wide active demethylation upon gamete fusion suggests inherited modified nucleosomal chromatin to act as a protective barrier. In agreement with this is the recent observation that CpG methylation levels of paternal PNs derived from injected round spermatids, which possess only nucleosomal chromatin and have high H4K8ac and H4K12ac levels (data not shown), are much higher than CpG levels of PNs derived from injected sperm (Kishigami et al., 2006).

Acetylation of paternal chromatin post-gamete fusion occurs in a stepwise fashion

Histone PTMs in the paternal chromatin prior to PN formation – i.e., the acetylations investigated here – evolve in three phases.

The transmission of H4K8ac and H4K12ac from the sperm constitutes the first phase. For H4K8ac, we unambiguously showed its transfer from the sperm nucleus to the zygote (Figs. 1A, B and Figs. 4.2B, B′). This is very likely also the case for H4K12ac since it is present in the chromocenter of caput sperm (Figs. 1J and 4.2C, C′).

The reason why, during male chromatin decondensation, the H4K12ac paternal modification cannot be distinguished from modification by the oocyte is the second phase that involves the deposition of maternally derived histones. Prior to deposition, histone H4 becomes acetylated at K5 and K12 (Sobel et al., 1995). Therefore, histone deposition will consequently obscure detection of H4K12ac-labeled paternally derived nucleosomes. Our earlier observation that maternal nucleosome deposition commences immediately after decondensation (van der Heijden et al., 2005) is in concordance with the synchronous accumulation of H4K5ac (Adenot et al., 1997) and H4K12ac (this study). It has been proposed (Adenot et al., 1997) that chromatin of type *a* sperm nuclei is hyperacetylated as indicated by the presence of H4K5ac. Although this may hold for somatic chromatin in interphase or mitosis, in the decondensing sperm chromatin, H4K5ac and H4K12ac are hallmarks of histone deposition and therefore precede subsequent acetylation or deacetylation events.

The third event occurs after full decondensation: H3K9K14ac, H3K18ac, H4K8ac and H4K16ac appear more or less synchronized (Figs. 1C and 2D′, G′, J′). A steady increase results in their homogeneous presence when recondensation commences (Figs. 1D and 2E′,H′,K′ and for a schematic overview, Fig. 5).

A possible function for hyperacetylation of paternal chromatin

Chromatin remodeling in elongating spermatids and in sperm nuclei after gamete fusion does involve similar histone PTMs, notwithstanding that the endpoints are opposite (i.e., from nucleosomes to protamines and vice versa). Both phases are characterized by a temporary hyperacetylated chromatin state. As mentioned earlier, in spermatid nuclei, this is thought to facilitate chromatin remodeling by decreasing nucleosome–DNA and nucleosome–nucleosome interactions (Oliva et al., 1987). Possibly, the physical changes conferred on nucleosomes by hyperacetylation facilitate fine-tuning of nucleosome position or density after their assembly. In general, acetylation of histone tails is associated with an enhanced transcriptional activity (Berger, 2002). Transcriptional activity in the male PN starts in mid-S phase, about 6 h after PN formation (Aoki et al., 1997). Since histone acetylation has a high turnover (Waterborg, 2002), a relation between early paternal chromatin acetylation and transcription status is disputable.

Phosphorylation of paternal histone H3 at serine 10, a conserved phenomenon

As in mouse, H3S10ph is also rapidly observed in *Xenopus* sperm after decondensation in egg extract (de la Barre et al., 2001), indicating that this phosphorylation event is evolutionary conserved. A function in chromatin condensation at mitosis has frequently been implied for this mark, although mutation of S10 does not affect this process (de la Barre et al., 2001). Phosphorylation of S10, therefore, does not cause chromatin condensation but seems to be a consequence (Prigent and Dimitrov, 2003). In the paternal zygotic chromatin, H3S10ph is homogeneously present when recondensation has started (Fig. 2B), again correlating chromatin condensation with this mark. An explanation for the

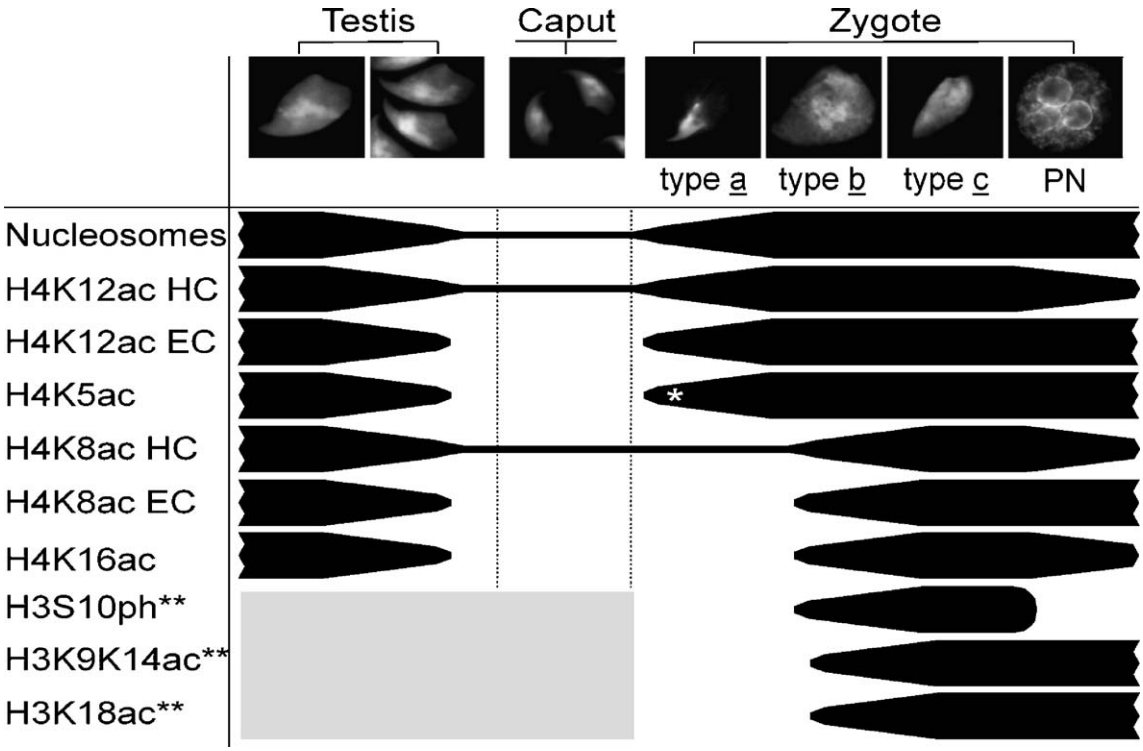

Fig. 5. Schematic overview of chromatin dynamics during spermiogenesis and in the early zygote. Presence of nucleosomes and PTMs during spermiogenesis, in sperm from the caput epididymis and in the early zygote up to 280 min post-insemination (~3.5 h after gamete fusion) is indicated with black bars. HC=heterochromatin, EC=euchromatin. * as shown in Adenot et al. (1997). **Since these histone PTMs were not detected in type *a* sperm nuclei, we did not determine their dynamics in spermiogenesis and caput sperm.

appearance of H3S10ph may be found in the fact that the sperm decondenses in a situation where Maturation Promoting Factor (MPF) is still present, until its activity decreases as a consequence of the end of telophase II (Verlhac et al., 1994). At that stage, a rapid maternal H3S10 dephosphorylation is observed (data not shown), while the paternal chromatin is accumulating this mark (Figs. 2A–B′). Maybe the paternal H3S10ph mark symbolizes the end of meiotic activity: it is rapidly removed at nuclear expansion due to PN formation (Fig. 2C).

Reestablishing the euchromatin–heterochromatin partition through localized deacetylation

After PN formation, loss of H4K8ac and H4K12ac is specifically observed in the centric chromatin (Figs. 1E and N). A potential role for this partial loss of H4K8ac and H4K12ac might be found in reestablishing the euchromatin–heterochromatin partition. Since the level of nucleosome acetylation has a direct effect on replication timing of DNA – lower acetylation levels delay and high levels stimulate replication (Kemp et al., 2005) – it is to be expected that these hypoacetylated chromatin domains will undergo delayed DNA replication. Centric DNA is typically late replicating in somatic cells. Although the male PN lacks most important hallmarks of heterochromatin (Cowell et al., 2002; Kourmouli et al., 2004; van der Heijden et al., 2005), in S phase in the mouse, zygote replication of euchromatin regions is followed by replication of heterochromatin domains (Aoki and Schultz, 1999). Since methylated CpGs are capable of recruiting HDAC containing complexes (Bird, 2002), the deacetylation of the paternal heterochromatin could be related to the retained CpG methylation in the heterochromatin (Santos et al., 2005). Thus, a decrease in acetylation of the zygotic paternal centric chromatin, possibly mediated through CpG methylation, will establish a somatic-like replication pattern. This separation in time of euchromatin and heterochromatin replication is expected to allow their further maturation by differential composition of the replication machinery (McNairn and Gilbert, 2003).

In summary, we show that centric heterochromatin is inherited from the father and is characterized by the presence of H4K8ac and H4K12ac. We propose this to be of significance for the reconstitution of soma-like male chromosomes after gamete fusion and possibly also for the conservation of CpG methylation. Furthermore, the dynamics of maternally derived histone PTMs indicate a facilitating role of hyperacetylation for chromatin remodeling in the pre-PN paternal chromatin while hypoacetylation of centric heterochromatin observed after PN formation could establish the euchromatin–heterochromatin partition as expressed by replication kinetics.

Acknowledgments

Dr. H. Stunnenberg (Department of Molecular Biology, NCMLS, Nijmegen, The Netherlands), Dr. P. Adams (FCCC, Philadelphia, PA), Dr. P. Singh (Division of Tumor Biology,

Department of Immunology and Cell Biology, Forschungszentrum Borstel, Germany), Dr. T. Jenuwein (IMP, Vienna, Austria), Dr. P. Burgoyne (Division of Stem Cell Research and Developmental Genetics, MRC National Institute for Medical Research, London, UK) and Dr. R. Balhorn (Electronic Engineering Technologies Division, Lawrence Livermore National Laboratory, Livermore, CA) are gratefully acknowledged for their antibodies. We thank Dr. D.G. Wansink (Dept. of Cell Biology, NCMLS, Nijmegen, The Netherlands) for critical reading of the manuscript. This research was financed by the Dutch Ministry of Health, Welfare and Sport.

Appendix A. Supplementary data

Supplementary data associated with this article can be found, in the online version, at doi:10.1016/j.ydbio.2006.06.051.

References

Adenot, P.G., Szollosi, M.S., Geze, M., Renard, J.P., Debey, P., 1991. Dynamics of paternal chromatin changes in live one-cell mouse embryo after natural fertilization. Mol. Reprod. Dev. 28, 23–34.

Adenot, P.G., Mercier, Y., Renard, J.P., Thompson, E.M., 1997. Differential H4 acetylation of paternal and maternal chromatin precedes DNA replication and differential transcriptional activity in pronuclei of 1-cell mouse embryos. Development 124, 4615–4625.

Aoki, E., Schultz, R.M., 1999. DNA replication in the 1-cell mouse embryo: stimulatory effect of histone acetylation. Zygote 7, 165–172.

Aoki, F., Worrad, D.M., Schultz, R.M., 1997. Regulation of transcriptional activity during the first and second cell cycles in the preimplantation mouse embryo. Dev. Biol. 181, 296–307.

Arney, K.L., Bao, S., Bannister, A.J., Kouzarides, T., Surani, M.A., 2002. Histone methylation defines epigenetic asymmetry in the mouse zygote. Int. J. Dev. Biol. 46, 317–320.

Baart, E.B., de Rooij, D.G., Keegan, K.S., de Boer, P., 2000. Distribution of Atr protein in primary spermatocytes of a mouse chromosomal mutant: a comparison of preparation techniques. Chromosoma 109, 139–147.

Berger, S.L., 2002. Histone modifications in transcriptional regulation. Curr. Opin. Genet. Dev. 12, 142–148.

Bird, A., 2002. DNA methylation patterns and epigenetic memory. Genes Dev. 16, 6–21.

Cowell, I.G., Aucott, R., Mahadevaiah, S.K., Burgoyne, P.S., Huskisson, N., Bongiorni, S., Prantera, G., Fanti, L., Pimpinelli, S., Wu, R., Gilbert, D.M., Shi, W., Fundele, R., Morrison, H., Jeppesen, P., Singh, P.B., 2002. Heterochromatin, HP1 and methylation at lysine 9 of histone H3 in animals. Chromosoma 111, 22–36.

de la Barre, A.E., Angelov, D., Molla, A., Dimitrov, S., 2001. The N-terminus of histone H2B, but not that of histone H3 or its phosphorylation, is essential for chromosome condensation. EMBO J. 20, 6383–6393.

de Lange, T., 2002. Protection of mammalian telomeres. Oncogene 21, 532–540.

Dyban, A.P., De Sutter, P., Verlinsky, Y., 1993. Okadaic acid induces premature chromosome condensation reflecting the cell cycle progression in one-cell stage mouse embryos. Mol. Reprod. Dev. 34, 402–415.

Haaf, T., Ward, D.C., 1995. Higher order nuclear structure in mammalian sperm revealed by in situ hybridization and extended chromatin fibers. Exp. Cell Res. 219, 604–611.

Hazzouri, M., Pivot-Pajot, C., Faure, A.K., Usson, Y., Pelletier, R., Sele, B., Khochbin, S., Rousseaux, S., 2000. Regulated hyperacetylation of core histones during mouse spermatogenesis: involvement of histone deacetylases. Eur. J. Cell Biol. 79, 950–960.

Hoyer-Fender, S., Singh, P.B., Motzkus, D., 2000. The murine heterochromatin protein M31 is associated with the chromocenter in round spermatids and is a component of mature spermatozoa. Exp. Cell Res. 254, 72–79.

Hunt, P., LeMaire, R., Embury, P., Sheean, L., Mroz, K., 1995. Analysis of chromosome behavior in intact mammalian oocytes: monitoring the segregation of a univalent chromosome during female meiosis. Hum. Mol. Genet. 4, 2007–2012.

Kemp, M.G., Ghosh, M., Liu, G., Leffak, M., 2005. The histone deacetylase inhibitor trichostatin A alters the pattern of DNA replication origin activity in human cells. Nucleic Acids Res. 33, 325–336.

Kim, J.M., Liu, H., Tazaki, M., Nagata, M., Aoki, F., 2003. Changes in histone acetylation during mouse oocyte meiosis. J. Cell Biol. 162, 37–46.

Kishigami, S., Van, T.N., Hikichi, T., Ohta, H., Wakayama, S., Mizutani, E., Wakayama, T., 2006. Epigenetic abnormalities of the mouse paternal zygotic genome associated with microinsemination of round spermatids. Dev. Biol. 289, 195–205.

Kourmouli, N., Jeppesen, P., Mahadevhaiah, S., Burgoyne, P., Wu, R., Gilbert, D.M., Bongiorni, S., Prantera, G., Fanti, L., Pimpinelli, S., Shi, W., Fundele, R., Singh, P.B., 2004. Heterochromatin and tri-methylated lysine 20 of histone H4 in animals. J. Cell Sci. 117, 2491–2501.

Kramers, K., Stemmer, C., Monestier, M., van Bruggen, M.C., Rijke-Schilder, T.P., Hylkema, M.N., Smeenk, R.J., Muller, S., Berden, J.H., 1996. Specificity of monoclonal anti-nucleosome auto-antibodies derived from lupus mice. J. Autoimmun. 9, 723–729.

Liu, L., Blasco, M., Trimarchi, J., Keefe, D., 2002. An essential role for functional telomeres in mouse germ cells during fertilization and early development. Dev. Biol. 249, 74–84.

Losman, M.J., Fasy, T.M., Novick, K.E., Monestier, M., 1992. Monoclonal autoantibodies to subnucleosomes from a MRL/Mp(−)+/+ mouse. Oligoclonality of the antibody response and recognition of a determinant composed of histones H2A, H2B, and DNA. J. Immunol. 148, 1561–1569.

McNairn, A.J., Gilbert, D.M., 2003. Epigenomic replication: linking epigenetics to DNA replication. BioEssays 25, 647–656.

Oliva, R., Bazett-Jones, D., Mezquita, C., Dixon, G.H., 1987. Factors affecting nucleosome disassembly by protamines in vitro. Histone hyperacetylation and chromatin structure, time dependence, and the size of the sperm nuclear proteins. J. Biol. Chem. 262, 17016–17025.

Palmer, D.K., O'Day, K., Margolis, R.L., 1990. The centromere specific histone CENP-A is selectively retained in discrete foci in mammalian sperm nuclei. Chromosoma 100, 32–36.

Peters, A.H., Plug, A.W., van Vugt, M.J., de Boer, P., 1997. A drying-down technique for the spreading of mammalian meiocytes from the male and female germline. Chromosome Res. 5, 66–68.

Peters, A.H., O'Carroll, D., Scherthan, H., Mechtler, K., Sauer, S., Schofer, C., Weipoltshammer, K., Pagani, M., Lachner, M., Kohlmaier, A., Opravil, S., Doyle, M., Sibilia, M., Jenuwein, T., 2001. Loss of the Suv39h histone methyltransferases impairs mammalian heterochromatin and genome stability. Cell 107, 323–337.

Peters, A.H., Kubicek, S., Mechtler, K., O'Sullivan, R.J., Derijck, A.A., Perez-Burgos, L., Kohlmaier, A., Opravil, S., Tachibana, M., Shinkai, Y., Martens, J.H., Jenuwein, T., 2003. Partitioning and plasticity of repressive histone methylation states in mammalian chromatin. Mol. Cell 12, 1577–1589.

Pittoggi, C., Renzi, L., Zaccagnini, G., Cimini, D., Degrassi, F., Giordano, R., Magnano, A.R., Lorenzini, R., Lavia, P., Spadafora, C., 1999. A fraction of mouse sperm chromatin is organized in nucleosomal hypersensitive domains enriched in retroposon DNA. J. Cell Sci. 112 (Pt. 20), 3537–3548.

Pivot-Pajot, C., Caron, C., Govin, J., Vion, A., Rousseaux, S., Khochbin, S., 2003. Acetylation-dependent chromatin reorganization by BRDT, a testis-specific bromodomain-containing protein. Mol. Cell. Biol. 23, 5354–5365.

Prigent, C., Dimitrov, S., 2003. Phosphorylation of serine 10 in histone H3, what for? J. Cell Sci. 116, 3677–3685.

Rousseaux, S., Caron, C., Govin, J., Lestrat, C., Faure, A.K., Khochbin, S., 2005. Establishment of male-specific epigenetic information. Gene 345, 139–153.

Russell, L.D., Ettlin, R.A., Hikim, A.P.S., Clegg, E.D., 1990. Histopathological Evaluation of the Testis. Cache River Press, Clearwater, FL.

Santos, F., Peters, A.H., Otte, A.P., Reik, W., Dean, W., 2005. Dynamic chromatin modifications characterise the first cell cycle in mouse embryos. Dev. Biol. 280, 225–236.

Singh, P.B., Georgatos, S.D., 2002. HP1: facts, open questions, and speculation. J. Struct. Biol. 140, 10–16.

Sobel, R.E., Cook, R.G., Perry, C.A., Annunziato, A.T., Allis, C.D., 1995. Conservation of deposition-related acetylation sites in newly synthesized histones H3 and H4. Proc. Natl. Acad. Sci. U. S. A. 92, 1237–1241.

Stein, P., Worrad, D.M., Belyaev, N.D., Turner, B.M., Schultz, R.M., 1997. Stage-dependent redistributions of acetylated histones in nuclei of the early preimplantation mouse embryo. Mol. Reprod. Dev. 47, 421–429.

Sterner, D.E., Berger, S.L., 2000. Acetylation of histones and transcription-related factors. Microbiol. Mol. Biol. Rev. 64, 435–459.

Sutovsky, P., Schatten, G., 2000. Paternal contributions to the mammalian zygote: fertilization after sperm–egg fusion. Int. Rev. Cytol. 195, 1–65.

Tagami, H., Ray-Gallet, D., Almouzni, G., Nakatani, Y., 2004. Histone H3.1 and H3.3 complexes mediate nucleosome assembly pathways dependent or independent of DNA synthesis. Cell 116, 51–61.

van der Heijden, G.W., Dieker, J.W., Derijck, A.A., Muller, S., Berden, J.H., Braat, D.D., van der Vlag, J., de Boer, P., 2005. Asymmetry in Histone H3 variants and lysine methylation between paternal and maternal chromatin of the early mouse zygote. Mech. Dev. 122, 1008–1022.

Verlhac, M.H., Kubiak, J.Z., Clarke, H.J., Maro, B., 1994. Microtubule and chromatin behavior follow MAP kinase activity but not MPF activity during meiosis in mouse oocytes. Development 120, 1017–1025.

Ward, W.S., Coffey, D.S., 1991. DNA packaging and organization in mammalian spermatozoa: comparison with somatic cells. Biol. Reprod. 44, 569–574.

Waterborg, J.H., 2002. Dynamics of histone acetylation in vivo. A function for acetylation turnover? Biochem. Cell Biol. 80, 363–378.

Widlund, H.R., Cao, H., Simonsson, S., Magnusson, E., Simonsson, T., Nielsen, P.E., Kahn, J.D., Crothers, D.M., Kubista, M., 1997. Identification and characterization of genomic nucleosome-positioning sequences. J. Mol. Biol. 267, 807–817.

Wright, S.J., 1999. Sperm nuclear activation during fertilization. Curr. Top. Dev. Biol. 46, 133–178.

Yang, X.J., 2004. Lysine acetylation and the bromodomain: a new partnership for signaling. BioEssays 26, 1076–1087.

Zalenskaya, I.A., Bradbury, E.M., Zalensky, A.O., 2000. Chromatin structure of telomere domain in human sperm. Biochem. Biophys. Res. Commun. 279, 213–218.